

 Open access • Journal Article • DOI:10.1103/PHYSREVLETT.42.1216

Measurement of fast-electron energy spectra and preheating in laser-irradiated targets

— [Source link](#) 

J. D. Hares, J. D. Kilkenny, M.H. Key, James G. Lunney

Institutions: Imperial College London, Queen's University Belfast

Published on: 30 Apr 1979 - Physical Review Letters (American Physical Society)

Topics: Energy (signal processing)

Related papers:

- [Theory of Hot-Electron Spectra at High Laser Intensity](#)
- [Observation of nonthermal energy distributions during the impulsive phase of solar flares](#)
- [Absorption of ultra-intense laser pulses.](#)
- [Hot-electron characterization from K \$\alpha\$ measurements in high-contrast, p-polarized, picosecond laser-plasma interactions](#)
- [Ignition and high gain with ultrapowerful lasers](#)

Share this paper:    

View more about this paper here: <https://typeset.io/papers/measurement-of-fast-electron-energy-spectra-and-preheating-4dryciskjd>

Measurement of Fast-Electron Energy Spectra and Preheating in Laser-Irradiated Targets

J. D. Hares and J. D. Kilkenny

Blackett Laboratory, Imperial College, London, United Kingdom

and

M. H. Key^(a) and J. G. Lunney

Department of Pure and Applied Physics, Queen's University, Belfast, Northern Ireland

(Received 12 February 1979)

Fast electrons produced by the irradiation of plane-layered targets with 20-J, 100-ps, 10^{15} -W-cm⁻², neodymium-laser pulses have been diagnosed by the $K\alpha$ emission which they cause at various depths in the targets. The fast-electron energy spectrum and absolute energy deposition (target preheat) are measured.

When high-intensity laser radiation is incident on a solid it is well known that the resulting plasma has both a thermal (cold) and a hot component in its electron velocity distribution and that a large fraction of the absorbed laser energy couples into the hot electrons.¹⁻³ Fast ions are accelerated by the hot electrons, and the temperature of the hot electrons T_H has been inferred from the ion-velocity spectrum.⁴ A substantial fraction of the hot-electron energy is transferred to the ions, and the remainder is deposited in the target causing preheating of the solid, x-ray continuum emission and K line emission. The hard-x-ray (5-50 keV) continuum slope has been widely used to estimate the hot-electron temperature.^{1,3,5} However, the experimental method is not amenable to spatial resolution, and the total energy inferred in the hot electrons is sensitive to the model electron distribution function.⁶

We report the first experiments using $K\alpha$ radiation from laser-produced plasmas to measure the magnitude of preheating of the solid by hot electrons, with radiation-induced $K\alpha$ emission and saturation of the $K\alpha$ emission due to ionization eliminated. The range and degree of the preheating, and the form of the hot-electron velocity distribution are also measured. Direct measurement of this preheating has not previously been obtained and is of importance for laser-fusion target design.

Earlier work^{7,8} has attributed $K\alpha$ emission to fast electrons and in a detailed study⁹ their range and effective temperature were deduced for 10.6- μ m radiation at 3×10^{13} W cm⁻². Target preheating was estimated in Ref. 8, but consideration of ionization effects below suggest that the conclusions drawn from the experiment were invalid.

$K\alpha$ radiation can arise from electron- or radiation-produced K -shell ionization. Radiative K -shell ionization is very efficient if the photon en-

ergy $h\nu$ is slightly greater than E_K the K -shell ionization potential. The low-energy x-ray recombination continuum from laser-produced plasmas has the form $I(\nu) = I_0 \exp(-h\nu/kT_c)$ where the cold-electron temperature T_c is ~ 0.5 keV in the present experiment. Thus to reduce radiation pumping E_K must be much greater than kT_c . In contrast, electrons are inefficient in K -shell ionization. The instantaneous ratio¹⁰ of K -shell ionization to total energy deposition by an electron of energy E may be written as

$$R(E) \sim 3.0 \times 10^{-2} \ln(E/E_K) / \ln(4E/\bar{E}_i)$$

for potassium, where the mean excitation energy \bar{E}_i is 240 eV. For $E > 15$ keV, $R(E)$ is nearly constant at $\bar{R} \approx 1\%$. The $K\alpha$ yield is then $\omega' \bar{R} U$ where U is the energy deposited by electrons, and ω' is the fluorescence yield times the $K\alpha$ photon energy divided by E_K (0.15 for Ca).

As U increases, the ionization causes only a small shift in the wavelength of the $K\alpha$ line until an electron is removed from the L shell,¹¹ when

$$U \equiv U_s = N_a \left\{ \sum_{n=1}^{Z-10} E_i^n + 1.5k[(Z-10)T_e + T_i] \right\},$$

where E_i^n is the ionization potential of ionization stage n and N_a is the number of fluor atoms under the focal area. The saturation energy yield of the "unshifted" $K\alpha$ line is simply $U_s \bar{R} \omega'$.

Previous work with neon⁸ has ignored this saturation effect.¹² We estimate the saturation energy of the electron-pumped neon $K\alpha$ in Ref. 8 to be 5×10^7 J (for 10^{14} atoms) compared with the reported observed yield of 2×10^4 J.

The saturation and radiation pumping effects suggest using a fluor whose Z is appreciably larger than 10, but not so large that E_K is comparable with kT_H . In the work below, Ca and K ($E_K = 4.04$ and 3.62 keV, respectively) were used and kT_H was 11 keV. A 20-J, 100-ps neodymium

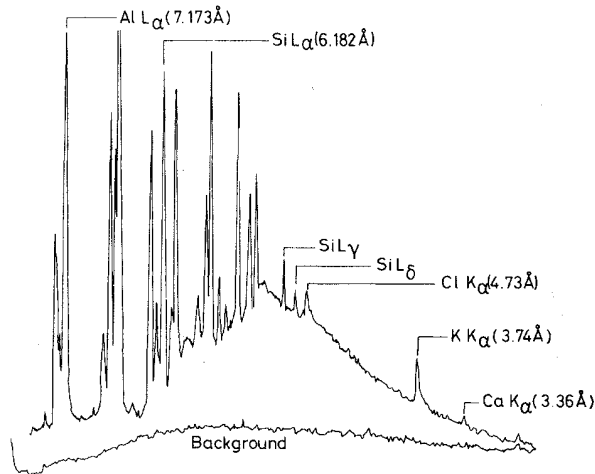


FIG. 1. A typical microdensitometer tracing from the front spectrometer. The Ca K α line appears much more brightly on the rear spectrometer, where it suffers no target absorption.

laser was normally incident on various plane-layered targets. The targets were positioned 150 μm away from the optimum focus of a $f/1$ lens. X-ray pinhole pictures indicated a focal spot of 100 μm , which corresponds to photographic measurements of the equivalent image plane. The layers were 0.1- μm Al; 1.0- μm SiO; 3.0- μm KCl; 2.5-, 12.5-, 25-, or 50- μm variable-thickness Mylar; and 2.5- μm CaF $_2$. The laser was incident on the Al. The top two layers of Al and SiO isolated the K α fluors from the ablation plasma, whose burnthrough depth for 100-ps pulse was only 0.1 μm . The Ca and K K α radiation was excited by electrons: The Cl with lower E_K was appreciably pumped by soft x-ray radiation. Time-integrated x-ray spectra were recorded by two miniature flat pentaerythritol crystal spectrometers. The reflectivities of the crystals have been measured.¹³ All the K α emission lines

were recorded by a spectrometer behind the targets. A spectrometer in front of the target recorded the K and Cl K α lines, the attenuated Ca K α line, and the soft-x-ray plasma emission.

A typical microdensitometer trace from the front spectrometer is shown in Fig. 1. Three K α lines, the plasma continuum, and the Si and Al plasma emission lines are shown. The Ca and K K α intensities for different Mylar thicknesses are shown in Fig. 2. As expected, with increasing Mylar thickness the number of electrons energetic enough to penetrate to the activate the rear fluor decreases and thus the K α yield decreases with increasing depth in target.

The saturation and radiation effects referred to above were experimentally demonstrated. Figure 3 shows the K α line profile from the K at the front, in which the energy deposition is highest. The line clearly has shifted components.¹¹ The energy in the "unshifted" component is $(1.4 \pm 0.1) \times 10^{-5} \text{ J sr}^{-1}$, whereas the energy in the shifted components is $(0.8 \pm 0.3) \times 10^{-5} \text{ J sr}^{-1}$: For K K α $U_s = 1.0 \times 10^{-5} \text{ J sr}^{-1}$ for the 100- μm -diam, 3- μm -deep emitting volume of KCl, in fair agreement with the experimental data.

To show the effect of radiation-induced K α emission, a 25- μm Mylar target with KCl on the rear was irradiated with a larger focal spot and hence lower flux density. There was no K K α yield observed, because the hot-electron temperature was too low. However, the Cl K α yield was $(1.3 \pm 0.1) \times 10^{-6} \text{ J sr}^{-1}$. The soft-x-ray recombination emission was the same as for the 100- μm focal spot, and was measured to have $I_0 = (6.0 \pm 1.0) \times 10^{-5} \text{ J sr}^{-1} \text{ eV}^{-1}$ and $kT_c = 0.5 \pm 0.1 \text{ keV}$. The calculated Cl K α yield induced by this recombination emission was $1.7 \times 10^{-6} \text{ J sr}^{-1}$, again in fair agreement with experiment. In this calculation proper account was taken of target geometry and reabsorption. The predicted radia-

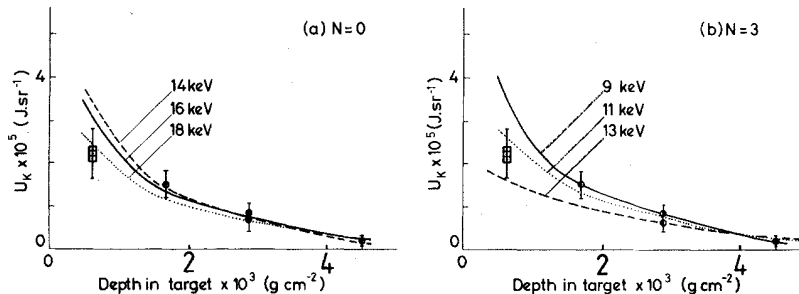


FIG. 2. Experimental and theoretical K α energies as a function of the average depth of the fluor layer in the target. Experimental energies are corrected for target absorption. Values of kT_H used for the theoretical curves are shown.

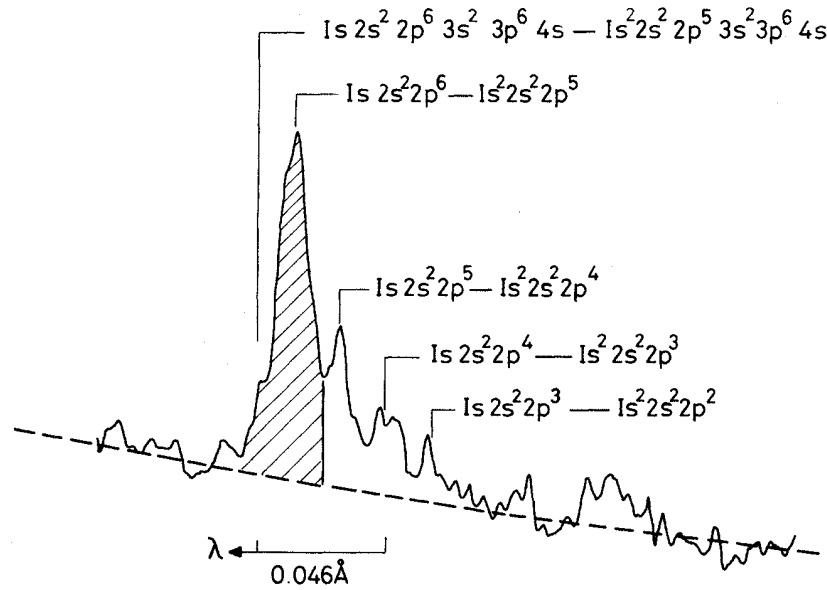


FIG. 3. An expanded microdensitometer tracing of a K $K\alpha$ line showing the short-wavelength shifted components. The indicated transitions from Ref. 11 should be compared with the observed peaks. "Unshifted" components are shaded.

tion pumped K $K\alpha$ yield is only $0.3 \times 10^{-6}\text{ J sr}^{-1}$ which is small compared with the lowest observed value of $2 \times 10^{-6}\text{ J sr}^{-1}$.

The energy spectrum of the fast electrons was obtained from calculations of the $K\alpha$ yield of monoenergetic electrons using Ref. 14. To check this calculation, especially at low energy, an electron beam was used to calibrate duplicate targets. The beam supplied $0.1\ \mu\text{A}$ at 15 to 50 kV into a $300\text{-}\mu\text{m}$ spot. The x-ray crystal spectrometer was used to record the various $K\alpha$

yields, for a known deposited charge. From the calibration and calculation the $K\alpha$ yields $Y(E)$ in $\text{J sr}^{-1}\text{ electron}^{-1}$ as a function of electron energy were obtained and are shown in Fig. 4. The agreement of the two adds confidence to our absolute measurement.

From the yields $Y(E)$ for monoenergetic electrons the yields for a distribution function $n(E)$ of electrons passing into the targets were predicted from $\int_0^\infty n(E)Y(E)dE$. With $n(E) = AE^{N/2} \exp(-E/kT_H)$, yields for $N=0$ and $N=3$ were calculated

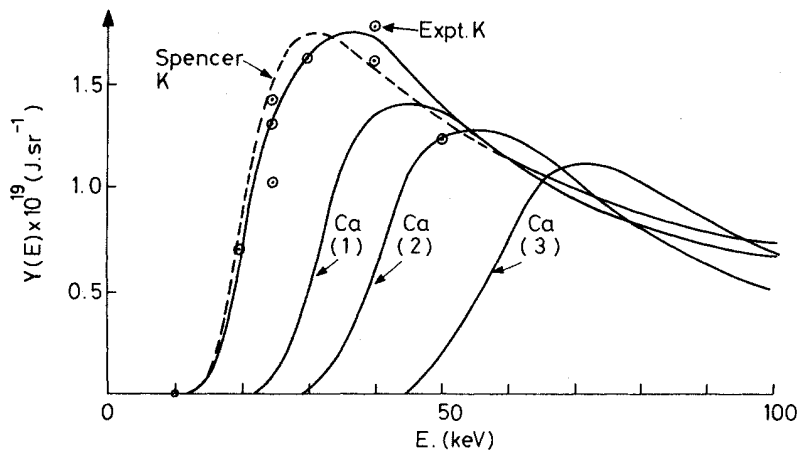


FIG. 4. The $K\alpha$ yield per electron as a function of incident electron energy for each of the different fluor layers. Curves 1, 2, and 3 refer to Mylar thicknesses of 2.5, 12.5, and $25.0\ \mu\text{m}$, respectively. The dotted line is the calculated yield for the front K layer and the points are from the electron-beam calibration. The good agreement should be noted. The solid lines are the yields used, derived from theory and the calibration.

TABLE I. Total energy deposition in fluor compounds.

Fluor layer (Mylar thickness)	Depth in target (mg cm ⁻²)	Deposited energy (J)	Deposited energy density (J cm ⁻³)
KCl (top)	0.56	0.40	1.4×10^7
CaF ₂ (2.5 μm)	1.58	0.24	1.0×10^7
CaF ₂ (12.5 μm)	2.81	0.12	5.1×10^6
CaF ₂ (25 μm)	4.50	0.04	1.7×10^6

and are shown in Fig. 2. The factors A and kT_H are determined by fitting the predicted yields to the experimental yields. The case $N=3$ fits the data best with $kT_H = 11 \pm 2$ keV. The slope of the hard-x-ray continuum between 10 and 20 keV also indicates a temperature of 12 ± 2 keV, which is comparable with collected data¹ at 2×10^{15} W cm⁻².

Choosing $N=3$, the fit to the experimental results gives $A = (9.4 \pm 2.0) \times 10^{11}$ electrons keV^{-2.5}, $kT_H = 11.0 \pm 2.0$ keV. The total energy in this distribution which is passing into the target is $\int_0^\infty n(E)E dE = 2.2 \pm 0.4$ J. However, the calculation of the energy deposited into the target is insensitive to the assumed distribution function, provided that the distribution is fitted to the observed yields. This is because $R(E)$ is almost constant and a simple division of the energy in the $K\alpha$ line by $\omega\bar{R}$ gives the total energy deposited in the fluor. A more accurate calculation of energy deposition has been made using the $N=3$ distribution and the results are shown in Table I.

Finally, we remark that the fast-electron energy deposition that we observe is broadly consistent with the expected overall energy balance. Of the 20 J onto the target, about 7 J should be absorbed.³ About 60% of the absorbed energy should reappear as fast ions.² We observe the bulk of the remainder as preheat. One might

speculate that this observed 2.2-J deposition of energy by hot electrons suggests that any inhibition of the hot-electron transport is not very significant.

We wish to acknowledge the contribution of P. T. Rumsby to target fabrication and of the staff of the Science Research Council Central Laser Facility. This work was supported by the Science Research Council, United Kingdom.

^(a) Present address: Science Research Council, Rutherford Laboratory, Chilton, Oxon, United Kingdom.

¹D. W. Forslund, J. M. Kindel, and K. Lee, Phys. Rev. Lett. **39**, 284 (1977).

²P. M. Campbell *et al.*, in *Proceedings of the Sixth International Conference on Plasma Physics and Controlled Nuclear Fusion Research, Birchesgaden, West Germany, 1976* (International Atomic Energy Agency, Vienna, 1977), Vol. I.

³E. K. Storm *et al.*, University of California Radiation Laboratory Report No. UCRL 50021-76, 1977 (unpublished), pp. 5.85-5.126.

⁴L. M. Wickens, J. E. Allen, and P. T. Rumsby, Phys. Rev. Lett. **41**, 243 (1978).

⁵J. W. Shearer *et al.*, Phys. Rev. A **6**, 764 (1972).

⁶K. A. Brueckner, Nucl. Fusion **17**, 1257 (1977).

⁷A. Zigler, H. Zmora, and J. L. Sczwab, Phys. Lett. **63A**, 275 (1977).

⁸B. Yaakobi, I. Pelah, and J. Hoose, Phys. Rev. Lett. **37**, 836 (1976).

⁹K. B. Mitchell and R. P. Godwin, J. Appl. Phys. **49**, 3851 (1977).

¹⁰*Handbook of Spectroscopy* (C.R.C. Press, Ohio, 1974), Vol. I.

¹¹L. L. House, Astrophys. J., Suppl. Ser. **18**, 21 (1969).

¹²B. Yaakobi, private communication.

¹³Rutherford Laboratory Central Laser Facility Annual Report No. RL-78-039, 1978 (unpublished).

¹⁴L. V. Spencer, *Energy Dissipation by Fast Electrons*, National Bureau of Standards Monograph No. I (U. S., GPO, Washington, D. C., 1959).